Navigating the Crowd: Non-linear MPC with Social Forces Dynamics for Human-Aware Robot Navigation

Stefano Trepella[1], Andrea Ostuni[1], Mauro Martini[1], Pablo Pueyo[2], Noé Pérez-Higueras[2], Marcello Chiaberge[1], Fernando Caballero[2], and Luis Merino[2]

***Abstract*— Safe and socially compliant navigation remains a fundamental challenge for autonomous robots operating in human-populated environments. Model Predictive Control (MPC) offers a robust alternative to classical and data-driven methods, although its effectiveness strongly depends on accurate human motion prediction and efficient computation. This paper introduces SFM-NMPC, a Social Force Model-based Non-linear MPC framework that embeds human motion prediction directly within the optimization loop. By incorporating the Social Force Model (SFM) into the dynamic model of surrounding agents, the controller jointly predicts human and robot trajectories over the prediction horizon, enabling socially-aware planning. A tailored set of social cost functions guides the optimization toward human-compliant behaviors. Despite the increased model complexity, the formulation runs in real time at 20 Hz. Extensive simulated testing in crowded environments demonstrates that SFM-NMPC outperforms state-of-the-art baselines in social compliance metrics while maintaining efficient and smooth navigation. An ablation study further highlights the contribution of the embedded SFM dynamics and social cost terms.**

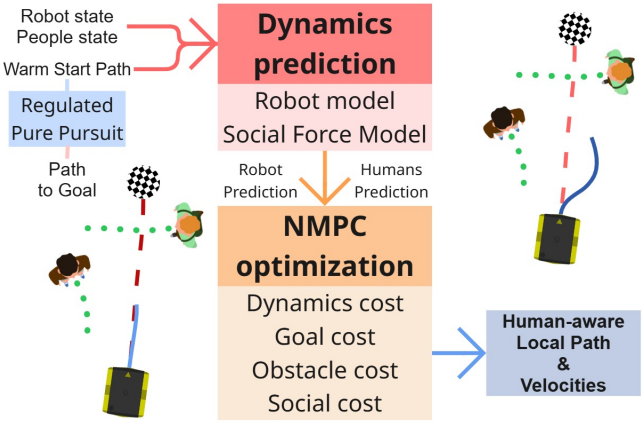

Fig. 1: SFM-NMPC embeds the Social Force Model in the prediction model of a Non-linear MPC controller as well as in the custom social cost terms to enhance human comfort and safety.

I. INTRODUCTION

Autonomous robots operating in real-world environments must navigate both efficiently and safely, especially when interacting with humans. Applications range from domestic robots [1] and healthcare assistants [2] to autonomous wheelchairs [3], making effective human-robot interaction models critical [4]. Robots must not only avoid physical obstacles [5] but also maintain appropriate distances, predict human movements, and avoid abrupt maneuvers. While Reinforcement Learning (RL) [6] and Deep Learning (DL) [7] can learn predictive behaviors, they require large datasets and substantial resources, and may lack transparency in safety-critical settings.

Model Predictive Control (MPC) [8] optimizes the robot trajectory over a finite horizon with real-time observations. Its key advantage is the ability to incorporate obstacle avoidance, velocity, and acceleration constraints within a unified framework. However, MPC must accurately predict human behavior, which is often precomputed even in existing social MPC formulations [9]. The Social Force Model (SFM) [10] models human motion as the result of social forces, goal attraction, and agent repulsion, and then provides an interpretable alternative to data-driven predictors.

We present SFM-NMPC[1], an efficient non-linear MPC that embeds the SFM in the dynamic model of people, jointly predicting human and robot trajectories within the optimization loop at 20 Hz. A custom set of social cost terms incorporating personal distance intrusion, relative headings, and social work derived from the SFM further guides the local planner. Fig. 1 summarizes the framework. Validation across diverse crowded environments demonstrates competitive advantages over multiple state-of-the-art baselines.

II. RELATED WORK

Human trajectory prediction has been incorporated into robot navigation to improve human comfort and safety through Gaussian Processes [11], Inverse Reinforcement Learning [12], and LSTMs [7]. Despite their sophistication, such methods often require extensive data and computational resources to run in real time on the robot. ORCA [13] is widely used for collision avoidance but treats people as moving obstacles, while the SFM [10] provides an interpretable, physics-inspired alternative that improves comfort and fluency in dense crowds [14], [15], [16]. In addition, other studies have included the SFM in the reward function for

This work was partially supported by the SWIch action (P.R. F.E.S.R.2021/27 - D.G.R. n.19-6962) within the EMPATHY project, and by PoliTO Interdepartmental Centre for Service Robotics (PIC4SeR). It is also partially supported by the project PICRAH4.0 (PLEC2023-010353) and INSERTION (PID2021-127648OB-C31), funded by the Spanish Research Agency and MCIN/AEI/10.13039/501100011033/FEDER, UE.

[1]Department of Electronics and Telecommunications, Politecnico di Torino, 10129, Torino, Italy. stefano.trepella@polito.it, andrea.ostuni@polito.it, mauro.martini@polito.it, marcello.chiaberge@polito.it

[2]School of Engineering, Pablo de Olavide University, Crta. Utrera km 1, Seville, Spain ppueyor@upo.es, noeperez@upo.es, fcaballero@upo.es, lmercab@upo.es

[1]https://anonymous.4open.science/r/sfm-nmpc-5A7C

Reinforcement Learning [17]. MPC-based pedestrian-aware planners [18], in contrast with the previous works, often rely on precomputed trajectory forecasts [9]. T-MPC++ [19] samples homotopy classes to select socially appropriate paths. SHINE [20] learns topologically distinct guidance trajectories, and deep residual learning has been used to improve efficiency with real crowd data [21]. An SFM-embedded MPC for crowded scenes exists [22], but treats human trajectories as fixed initial predictions. Our approach integrates the SFM dynamically within the MPC optimization loop, co-propagating human and robot trajectories at each step alongside custom social cost terms, achieving real-time performance while remaining interpretable and scalable.

III. METHODOLOGY

In this section, the proposed SFM-NMPC framework is formally presented. First, we define the adopted MPC formulation, the state and dynamics models used to propagate the prediction forward. Then, all the terms of the cost function are explained in detail. Finally, the overall optimization loop mechanism is described.

A. Adopted MPC Formulation

We propose a local planner based on Non-linear MPC (NMPC) with a discrete-time direct formulation. Given robot pose $\mathbf{p}_i^R \in SE(2)$ and control vector $\mathbf{u}_i \in \mathbb{R}^2$ (linear and angular velocities), the unicycle kinematic model propagates the robot via Euler integration:

$$\mathbf{p}_{i+1}^R = \mathbf{p}_i^R + \mathbf{G}(\theta_i)\mathbf{u}_i \Delta t_s \tag{1}$$

where Δt_s is the prediction time step and $\mathbf{G}(\theta_i)$ is the input mapping matrix derived from the continuous transient function g_t. Crucially, in our work, the optimized robot pose $\mathbf{p}_i^R$ also drives the SFM prediction of surrounding agents. For every agent k in the set $\mathcal{A}$, the velocity $\mathbf{v}_i^{A_k}$ is updated by integrating the sum of acting forces (Fig. 2):

$$\mathbf{v}_{i+1}^{A_k} = \mathbf{v}_i^{A_k} + \left(\mathbf{F}_{soc}(\mathbf{p}_i^R, \mathbf{p}_i^{A_k}) + \mathbf{F}_{drive}(\mathbf{v}_i^{A_k})\right) \Delta t_s \tag{2}$$

where $\mathbf{F}_{soc}$ is the repulsive interaction force and $\mathbf{F}_{drive}$ is a relaxation force. The repulsive force follows the Helbing formulation:

$$\mathbf{F}_{soc} = A_{soc}(f_v \mathbf{n}_D + f_\theta \mathbf{n}_\perp) \tag{3}$$

with $\mathbf{n}_D$ derived from $\mathbf{D} = \lambda(\mathbf{v}_i^R - \mathbf{v}_i^{A_k}) + \mathbf{n}_{ra}$, coupling relative velocity and the robot-to-agent unit direction. The scalars f_v and f_θ are exponential decay functions of the Euclidean distance $\|\mathbf{r}_{ra}\|$ and angular displacement θ. Agent positions are advanced via Semi-Implicit Euler integration:

$$\mathbf{p}_{i+1}^{A_k} = \mathbf{p}_i^{A_k} + \mathbf{v}_{i+1}^{A_k} \Delta t_s \tag{4}$$

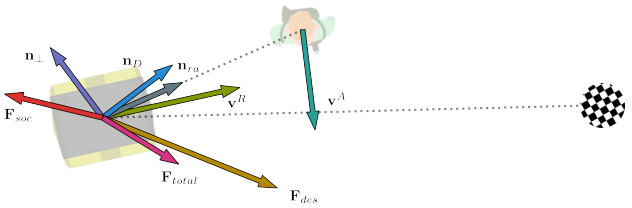

Fig. 2: The diagram of the social forces considered by the SFM [10].

B. Cost Function

The set of velocity commands χ is optimized by solving a non-linear least-squares (NLS) problem using Ceres [23]:

$$\begin{aligned}
\chi^* = \min_{\chi} J(\chi) &:= J_{\text{obs}} + J_{\text{goal}} + J_{\text{dyn}} + J_{\text{soc}} \\
\text{s.t.} \quad \mathbf{p}_{i+1}^R &= \mathbf{p}_i^R + \mathbf{G}(\theta_i)\mathbf{u}_i \Delta t_s && \forall i = 0,\dots,N_p \\
\mathbf{p}_{i+1}^{A_k} &= \mathbf{p}_i^{A_k} + \mathbf{v}_{i+1}^{A_k} \Delta t_s && \forall k \in \mathcal{A}, \forall i = 0,\dots,N_p \\
\mathbf{v}_{i+1}^{A_k} &= \mathbf{v}_i^{A_k} + (\mathbf{F}_{soc} + \mathbf{F}_{drive}) \Delta t_s && \forall k \in \mathcal{A}, \forall i = 0,\dots,N_p - 1 \\
v_{\text{lb}} \le v_i \le v_{\text{ub}} \quad & \omega_{\text{lb}} \le \omega_i \le \omega_{\text{ub}} && \forall i = 0,\dots,N_p - 1
\end{aligned} \tag{5}$$

N_p represents the prediction horizon, and the robot velocities are bounded between independent lower and upper bounds for the linear v and angular velocities.

$J(\chi)$ in Eq. 5 represents the sum of different costs to be considered; these represent the competing objectives, and each term is weighted by a different factor α, aiming to balance obstacle avoidance, social behavior, and smooth trajectories. J_{obs} penalizes proximity to obstacles via bi-cubic interpolation on a $6 \times 6\,\text{m}$ local costmap. J_{goal} encompasses path-following, path-alignment, goal-alignment, and goal-reaching terms. J_{dyn} promotes smooth trajectories by penalizing deviations from a desired speed and limiting acceleration. The social component J_{soc} comprises three terms:

1) Proxemics cost: J_ρ penalizes proximity to agents via exponential decay over all visible agents:

$$J_\rho = \alpha_\rho \sum_{i=1}^{N_p} \sum_{k=1}^{\mathcal{N}_\mathcal{A}} \beta \cdot \exp\left(-\frac{\|\mathbf{p}_{xy,i}^R - \mathbf{p}_{xy,i}^{A_k}\|^2}{d_0^2} \right) \tag{6}$$

where d_0 is the characteristic proxemic distance and β is a scaling factor.

2) Social Work: J_{work} minimizes the social force exerted by the robot on agents:

$$J_{\text{work}} = \alpha_{\text{work}} \sum_{i=1}^{N_p} \left(\sum_{k=1}^{\mathcal{N}_\mathcal{A}} \|\mathbf{F}_{robot \to agent_k}\|^2 \right) \tag{7}$$

derived from the Helbing formulation of the SFM [10].

3) Heading social cost: $J_{s\theta} = J_{s\theta\text{long}} + J_{s\theta\text{cross}}$ promotes predictive, socially compliant robot heading. $J_{s\theta\text{long}}$ penalizes heading toward or alongside the nearest agent k^*:

$$\begin{aligned}
J_{\text{s}\theta\text{long}} = \alpha_{\text{s}\theta} \sum_{i=1}^{N_p} e^{-d^2/d_s^2} \cdot \Big(& \underbrace{\text{sp}\big(\cos(\theta_i - \phi_{k^*})\big)}_{\text{position alignment}} + \\
& \alpha_v \cdot \underbrace{\text{sp}\big(\cos(\theta_i - \psi_{k^*})\big)}_{\text{velocity alignment}} \Big)
\end{aligned} \tag{8}$$

where sp is the Softplus function. $J_{s\theta\text{cross}}$ addresses perpendicular crossing with a speed and a steering penalty:

$$J_{s\theta\text{cross}} = \alpha_{\text{cross}} \sum_{i=1}^{N_p} e^{-d^2/d_s^2} \Big(\underbrace{v_i \cdot \sin^2(\theta_i - \psi_{k^*})}_{\text{speed penalty}} + \underbrace{\alpha_{\text{bear}} \cdot \text{sp}\big(\text{c} \cdot \omega_i \cdot s\big) \cdot \sin^2(\theta_i - \psi_{k^*})}_{\text{steering penalty}} \Big), \tag{9}$$

where $\mathbf{c} = \mathbf{n}_{ra} \times \mathbf{n}_{\psi}$ indicates whether the agent crosses from the left or right, and penalizes turning in the wrong direction.

C. Optimization Loop

Algorithm 1: SFM Non-linear MPC

Input : $\mathcal{P}_{global}$, $\mathcal{M}_{local}$, $\mathcal{A}$, p_0, $\mathcal{T}_{prev}$, χ_{prev}
Output: $\{\chi^*, \mathcal{T}^*\}$
Compute reference trajectories with $(\mathcal{T}_{ref}, U_{ref}) = RPP(P_{global}, L_d, p_0)$
Warm-start control sequence $\chi_0 = (U_{ref}, \chi_{prev})$
Warm-start trajectory $\mathcal{T}_0 = (\mathcal{T}_{ref}, \mathcal{T}_{prev})$
Build the cost function in Eq.5 and propagate the robot pose and the agents forward using the SFM.
Solve the non-linear least-squares problem with Ceres starting from χ_0 and $\mathcal{T}_0$ to obtain χ^*
Roll out $\mathcal{T}^*$ by forward-propagating p_0 with χ^*
return $(\chi^*, \mathcal{T}^*)$

A Regulated Pure Pursuit (RPP) algorithm extracts a local reference trajectory $\mathcal{T}_{ref}$, and initial control inputs U_{ref} from the global path $\mathcal{P}_{global}$ using robot pose $\mathbf{p}_0$ and a dynamic lookahead distance L_d. The optimizer warm-starts using a blend of U_{ref} and the previous solution χ_{prev} (weighted by α_{com}), then solves the NLS problem at 20 Hz following the receding-horizon principle. A control horizon T_c and block length B reduce computational cost. The prediction horizon is set to $T_p = 2\,\text{s}$ with $\Delta t_s = 0.1\,\text{s}$.

IV. Evaluation Methodology

A. Environments and Settings

We evaluated SFM-NMPC and six state-of-the-art baselines using HuNavSim [24] in Gazebo across two environments (Fig. 3): an open-space map with crossing, passing, and crowded-navigation scenarios (4–8 pedestrians), and a mixed indoor map with corridors, narrow passages, and rooms. Each algorithm was run 30 times per scenario.

B. Baselines

- MPPI_{GSC}: MPPI [25] from Nav2 [26] with Gaussian social costmap [27];
- DWB_{GSC}: Dynamic Window Approach [5] from Nav2 with Gaussian social costmap;
- ORCA: Optimal Reciprocal Collision Avoidance [13];
- SARL: Socially Attentive Reinforcement Learning [6];
- Pure SFM: robot velocity driven by SFM forces [10];

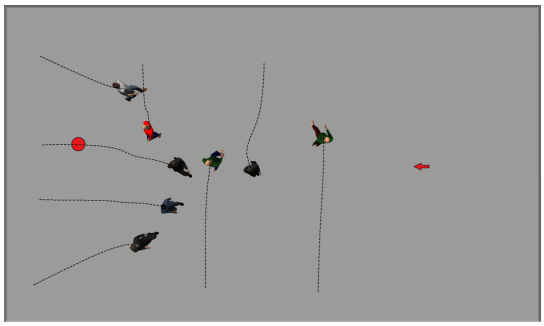

(a) World 1 – Open space.

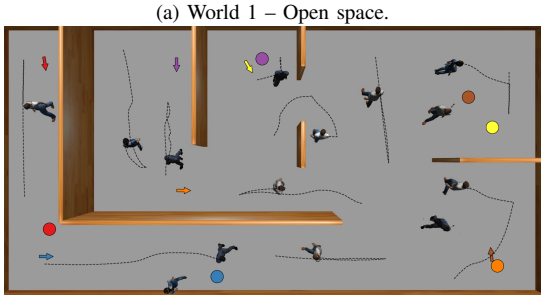

(b) World 2 – Corridors, rooms, and narrow passages.

Fig. 3: Maps used for evaluation with robot and human trajectories.

- NMPC: our NMPC without SFM dynamics or social costs.

All were implemented as Nav2 controller plugins with a shared A* global planner and costmaps; local controllers run at 20 Hz.

C. Evaluation Metrics

Navigation performance is assessed via success rate (SR), path length (PL), and time to goal (TTG). Social compliance is measured by social work per step (SW_{step})—the average SFM force generated along the trajectory—and the average minimum distance to the nearest person (AMD).

V. Results

TABLE I
SUMMARY OF SOCIAL NAVIGATION METRICS FOR EACH NAVIGATOR IN THE MIXED AND OPEN SPACE SCENARIOS, AS WELL AS OVERALL.

Map	Method	SR (%) ↑	PL (m) ↓	TTG (s) ↓	SW_{step} ↓	AMD (m) ↑
Mixed	DWB_{GSC}	42.00	9.04	14.27	16.02	0.99
	MPPI_{GSC}	91.00	9.28	16.56	13.48	1.00
	ORCA	16.00	**5.99**	**10.45**	19.90	0.98
	Pure SFM	31.00	17.34	31.43	13.80	**1.02**
	SARL	46.00	7.98	11.91	17.19	0.93
	NMPC	81.00	9.26	16.50	13.27	0.88
	SFM-NMPC	**97.00**	9.96	18.70	**11.96**	0.99
Open Space	DWB_{GSC}	**100.00**	**10.36**	**15.83**	9.96	1.60
	MPPI_{GSC}	99.00	10.56	17.57	9.83	1.52
	ORCA	81.00	11.71	26.39	9.10	1.63
	Pure SFM	**100.00**	11.00	17.47	9.73	1.71
	SARL	96.00	15.94	29.47	**8.04**	1.70
	NMPC	**100.00**	10.88	16.73	10.27	1.53
	SFM-NMPC	**100.00**	11.13	18.17	8.17	**1.73**
Overall	DWB_{GSC}	70.00	**9.54**	**14.86**	14.00	1.19
	MPPI_{GSC}	94.00	9.71	16.90	12.26	1.17
	ORCA	38.00	10.28	22.41	16.30	1.20
	Pure SFM	54.00	14.62	25.45	12.44	**1.25**
	SARL	62.00	11.96	20.69	14.14	1.18
	NMPC	87.00	9.87	16.59	12.27	1.10
	SFM-NMPC	**98.00**	10.35	18.52	**10.70**	1.24

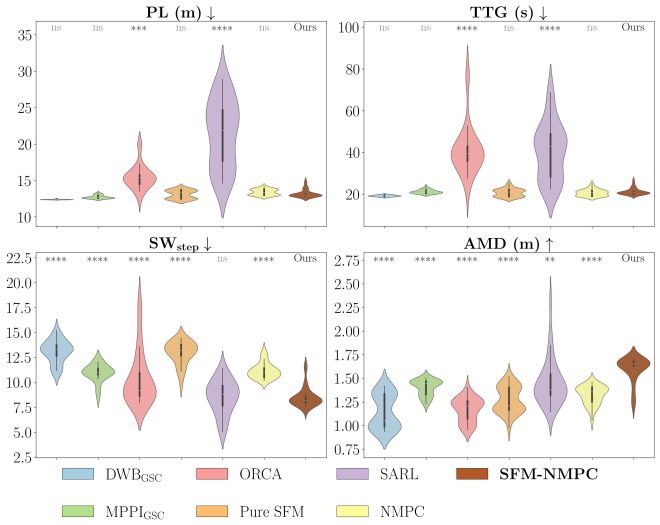

Fig. 4: Violin plots on the open-space environment. SFM-NMPC achieves the best social behavior while maintaining navigation efficiency. Asterisks indicate Tukey HSD p-value thresholds.

A. Quantitative Results

Table I summarizes average metrics across both maps. In open space, all methods achieve high SR, but SFM-NMPC obtains the best AMD and second-best SW_{step}. The better SW_{step} of SARL must be interpreted alongside its substantially longer path and traversal time (nearly twice the TTG), reflecting the oscillatory behavior typical of RL policies. ORCA's SR is the lowest across both maps. In the challenging mixed indoor scenarios, most baselines fail due to collisions; SFM-NMPC and $\mathrm{MPPI}_{\mathrm{GSC}}$ are the top-performing methods, confirming the advantage of model-predictive approaches when fast reaction to moving agents is critical. The basic NMPC also performs robustly in navigation success; adding SFM dynamics and social costs yields the best overall SW_{step}. Fig. 4 shows metric distributions with pairwise Tukey HSD significance tests, confirming consistent improvement in social compliance.

B. Proxemics

Fig. 5 shows the percentage of time spent intruding into intimate, personal, social, and public zones. SFM-NMPC achieves the lowest intimate-space intrusion overall and is comparable to Pure SFM in mixed scenes. In open space, model predictive-based planners (MPPI, NMPC, SFM-NMPC) reduce intimate intrusions to nearly zero.

C. Ablation Study

Fig. 6 shows the incremental effect of each social cost term. NMPC alone achieves efficient navigation, but with the worst social impact. Adding J_ρ and J_{work} yields gradual improvements in SW_{step} and AMD. The largest boost in both median performance and robustness comes from the heading cost $J_{s\theta}$, which also improves navigation efficiency. This confirms that the proposed cost formulation is modular and independently beneficial regardless of the dynamics model.

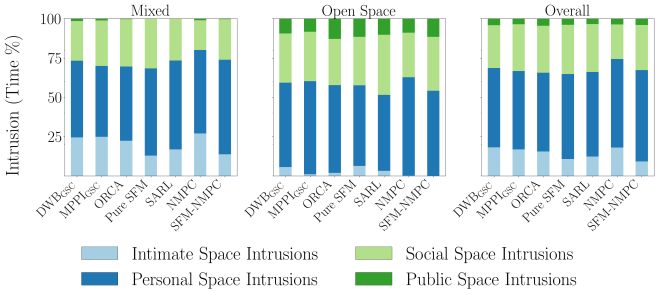

Fig. 5: Proxemics metrics across Mixed, Open Space, and Overall scenarios.

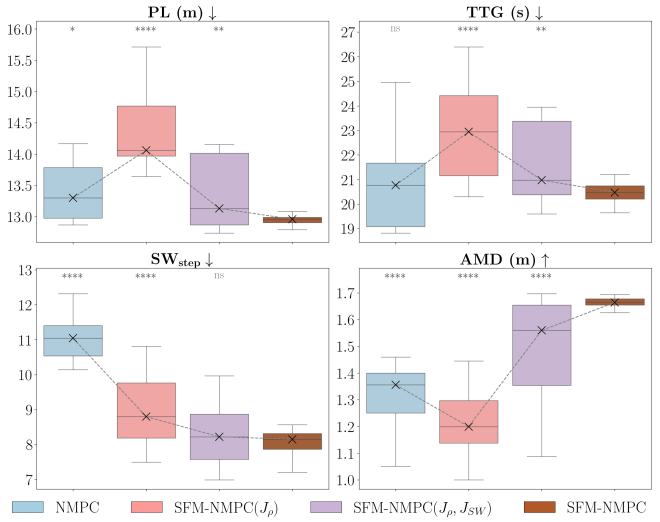

Fig. 6: Ablation study box plots on the open-space crowded environment. Asterisks indicate Tukey HSD p-value thresholds.

VI. CONCLUSIONS

This paper presented SFM-NMPC, a non-linear MPC framework for socially aware robot navigation that integrates the Social Force Model directly into the prediction and optimization loop. By jointly predicting robot and human trajectories at 20 Hz, the controller achieves interpretable, real-time socially compliant planning without relying on precomputed trajectories or data-driven predictors. Tailored social cost terms further improve compliance without sacrificing navigation efficiency. Extensive validation across diverse crowded scenarios confirmed improvements over competitive baselines on social metrics. Future work will validate SFM-NMPC on a real robot under perception uncertainty and explore co-optimization of robot and human trajectories.

REFERENCES

[1] A. Eirale, M. Martini, L. Tagliavini, D. Gandini, M. Chiaberge, and G. Quaglia, "Marvin: An innovative omni-directional robotic assistant for domestic environments," *Sensors*, vol. 22, no. 14, p. 5261, 2022.

[2] J. Holland, L. Kingston, C. McCarthy, E. Armstrong, P. O'Dwyer, F. Merz, and M. McConnell, "Service robots in the healthcare sector," *Robotics*, vol. 10, no. 1, p. 47, 2021.

[3] Y. Morales, T. Miyashita, and N. Hagita, "Social robotic wheelchair centered on passenger and pedestrian comfort," *Robotics and Autonomous Systems*, vol. 87, pp. 355–362, 2017.

[4] R. Hussain and S. Zeadally, "Autonomous cars: Research results, issues, and future challenges," *IEEE Communications Surveys & Tutorials*, vol. 21, no. 2, pp. 1275–1313, 2018.

[5] D. Fox, W. Burgard, and S. Thrun, "The dynamic window approach to collision avoidance," *Robotics & Automation Magazine, IEEE*, vol. 4, pp. 23 – 33, 04 1997.

[6] K. Li, Y. Xu, J. Wang, and M. Q.-H. Meng, "Sarl: Deep reinforcement learning based human-aware navigation for mobile robot in indoor environments," in *2019 IEEE International Conference on Robotics and Biomimetics (ROBIO)*, 2019, pp. 688–694.

[7] A. Alahi, K. Goel, V. Ramanathan, A. Robicquet, L. Fei-Fei, and S. Savarese, "Social lstm: Human trajectory prediction in crowded spaces," in *Proceedings of the IEEE conference on computer vision and pattern recognition*, 2016, pp. 961–971.

[8] P. Falcone, F. Borrelli, J. Asgari, H. E. Tseng, and D. Hrovat, "Predictive active steering control for autonomous vehicle systems," *IEEE Transactions on control systems technology*, vol. 15, no. 3, pp. 566–580, 2007.

[9] M. Everett, Y. F. Chen, and J. P. How, "Motion planning among dynamic, decision-making agents with deep reinforcement learning," in *IROS*, 2018.

[10] Helbing and Molnár, "Social force model for pedestrian dynamics." *Physical review. E, Statistical physics, plasmas, fluids, and related interdisciplinary topics*, vol. 51 5, pp. 4282–4286, 1995.

[11] D. Ellis, E. Sommerlade, and I. Reid, "Modelling pedestrian trajectory patterns with gaussian processes," in *2009 IEEE 12th international conference on computer vision workshops, ICCV workshops*. IEEE, 2009, pp. 1229–1234.

[12] B. D. Ziebart, N. Ratliff, G. Gallagher, C. Mertz, K. Peterson, J. A. Bagnell, M. Hebert, A. K. Dey, and S. Srinivasa, "Planning-based prediction for pedestrians," in *2009 IEEE/RSJ International Conference on Intelligent Robots and Systems*. IEEE, 2009, pp. 3931–3936.

[13] J. Van den Berg, M. Lin, and D. Manocha, "Reciprocal velocity obstacles for real-time multi-agent navigation," in *2008 IEEE international conference on robotics and automation*. Ieee, 2008, pp. 1928–1935.

[14] A. Bera, S. Kim, T. Randhavane, S. Pratapa, and D. Manocha, "Glmp-realtime pedestrian path prediction using global and local movement patterns," in *2016 IEEE International Conference on Robotics and Automation (ICRA)*. IEEE, 2016, pp. 5528–5535.

[15] A. Rudenko, L. Palmieri, M. Herman, K. M. Kitani, D. M. Gavrila, and K. O. Arras, "Human motion trajectory prediction: A survey," *The International Journal of Robotics Research*, vol. 39, no. 8, pp. 895–935, 2020.

[16] Y. Gao and C.-M. Huang, "Evaluation of socially-aware robot navigation," *Frontiers in Robotics and AI*, vol. 8, p. 721317, 2022.

[17] M. Martini, N. Pérez-Higueras, A. Ostuni, M. Chiaberge, F. Caballero, and L. Merino, "Adaptive social force window planner with reinforcement learning," in *2024 IEEE/RSJ International Conference on Intelligent Robots and Systems (IROS)*. IEEE, 2024, pp. 4816–4822.

[18] D. Q. Mayne, J. B. Rawlings, C. V. Rao, and P. O. M. Scokaert, "Constrained model predictive control: Stability and optimality," *Automatica*, 2000.

[19] H. De Groot, J. Smith, and W. Li, "Topology-driven model predictive control for safe navigation in dynamic environments," in *IEEE International Conference on Robotics and Automation (ICRA)*, 2024, pp. 1234–1240.

[20] D. Martinez-Baselga, O. de Groot, L. Knoedler, L. Riazuelo, J. Alonso-Mora, and L. Montano, "Shine: Social homology identification for navigation in crowded environments," *The International Journal of Robotics Research*, vol. 45, no. 1, pp. 60–79, 2026. [Online]. Available: https://doi.org/10.1177/02783649251344639

[21] J. R. Han, H. Thomas, J. Zhang, N. Rhinehart, and T. D. Barfoot, "Dr-mpc: Deep residual model predictive control for real-world social navigation," *IEEE Robotics and Automation Letters*, 2025.

[22] E. Fiasché, P. Martinet, and E. Malis, "Towards autonomous robot navigation in human populated environments using an universal sfm and parametrized mpc," in *2023 IEEE/RSJ International Conference on Intelligent Robots and Systems (IROS)*. IEEE, 2023, pp. 7422–7427.

[23] S. Agarwal, K. Mierle, and T. C. S. Team, "Ceres solver," 10 2023. [Online]. Available: https://github.com/ceres-solver/ceres-solver

[24] N. Pérez-Higueras, R. Otero, F. Caballero, and L. Merino, "Hunavsim: A ros 2 human navigation simulator for benchmarking human-aware robot navigation," *IEEE robotics and automation letters*, vol. 8, no. 11, pp. 7130–7137, 2023.

[25] G. Williams, A. Aldrich, and E. A. Theodorou, "Model predictive path integral control using covariance variable importance sampling," *CoRR*, vol. abs/1509.01149, 2015. [Online]. Available: http://arxiv.org/abs/1509.01149

[26] S. Macenski, F. Martín, R. White, and J. G. Clavero, "The marathon 2: A navigation system," in *2020 IEEE/RSJ International Conference on Intelligent Robots and Systems (IROS)*. IEEE, 2020, pp. 2718–2725.

[27] "NAV2 social costmap plugin ros2," https://github.com/robotics-upo/nav2_social_costmap_plugin, accessed: 2026-03-02.